Vibration and Acoustics Research Journal
Vol. 1, No. 1; 2019
Published by CanSRG
http://cansrg.com/journals/varj/

The Influence of the Traveling Waves on the Dynamic Behavior of Beams

Tassos P. Avraam and George T. Michaltsos*
National Technical University of Athens, Athens, Greece

Abstract

Evolution of trains and achievement of very high speeds led researchers to study the influence of these speeds on the dynamic behavior of technical works that undergo developed stresses. In this paper, the effect of the traveling waves on the dynamic behavior of a bridge or of a beam on elastic foundation was studied. Using the results obtained in our previous publication i.e. the formulae giving the expressions of eigenfrequencies and of shape functions, we used the complete model, which is governed by Timoshenko's equation for the study of the forced motion of a bridge or of a beam on elastic foundation under the action of moving loads with regular to very high speeds. A 2-DOF model is considered for the solution of the bridge or the beam while the theoretical formulation is based on the continuum approach which has been used in literature to analyze such bridges.

Keywords: *Wave propagation; Bridges' dynamic; Critical speeds; Traveling waves.*

Nomenclature

A	the cross sectional area	t	time
b	beam with	Tn	time function
E	modulus of elasticity	υ_M, υ_Q	moment and shear velocities of waves, respectively
G	shear modulus of elasticity	w	beam deformation
J	moment of inertia	β	damping coefficient
k	Winkler's factor	λ	beam slenderness ratio
k'	Timoshenko's shear coefficient	ρ	specific weight of beam
L	beam length	X_n	shape function
m	mass per unit length	ω_n	eigenfrequencies
p	the external loading		

1. Introduction

This paper is the sequel of paper [1], in which the influence of traveling waves on eigenfrequencies and critical speeds on a bridge or a beam on elastic foundation was studied. Many solution techniques have been reported [1-10] for structures with specific geometrical characteristics and finite, periodic or semi-infinite boundary conditions.

Many research papers use F.E.M. to analyze the influence of waves on an elastic solid [11-16], while several researchers studied this problem through experimental investigation [17-24]. Among many frequency domain methods, the spectral element method has been proved suitable for analysis of waves' propagation in real engineering structures. This spectral element method uses the exact solution of differential equations which governs the problem.

It has to be mentioned that there are studies on the behavior of traveling waves in various conditions such as the propagation along a rough thin-elastic beam or the study of the reflection and transmission of waves on an elastic beam [25,27]. Lastly, a lot of researchers studied the influence of the wave propagation on plates [28], underground power houses [29], concrete bridges [30], metal beams [31] and cable-stayed bridges [32].

* Corresponding Author
Submitted: September 16, 2019 Accepted: December 22, 2019

Flügge demonstrated [33], that an impulsive disturbance on a beam involving both shear and moment will result in two wave trains, i.e. one that propagates with the shear wave velocity $\upsilon_Q = \sqrt{k'G/\rho}$ and another that propagates with the moment-wave velocity $\upsilon_M = \sqrt{E/\rho}$ along the beam (ρ being the mass per unit volume, and k' the corrective shear coefficient of Timoshenko [35, 36, 37]). It has been observed that if the cross-section of a beam is such to have $k'G = E$, then the velocities υ_Q and υ_M will be equal and the two types of disturbances will travel together. In general, these two types of disturbance will travel with different velocities.

To study the aforementioned very interesting problems, numerous mechanical models of beams have been presented. Three mechanical models of beams have been presented in which the main parameters are the lumped masses. These models were first proposed and studied by Schirmer [34].

In this paper the effect of the traveling waves on the dynamic behavior of a bridge or of a beam on elastic foundation is studied. Using the results obtained in [1] i.e. the formulae giving the expressions of eigenfrequencies and of shape functions, we use the complete model which is governed by Timoshenko's equation for the study of the forced motion of a bridge or of a beam on elastic foundation under the action of moving loads moved with regular to very high speeds.

The evolution of trains and the achievement of very high speeds lead researchers to study the influence of these speeds on the dynamic behavior of the technical works that undergoing the developed stresses. A 2-DOF model is considered for the solution of the bridge or the beam while the theoretical formulation is based on the continuum approach which has been used in literature to analyze such bridges. Analytical results are presented in graphical form (plots and diagrams) showing the influence of traveling waves on the dynamic deflection of a bridge made from steel or concrete. Lastly a finite beam on elastic foundation of Winkler type is also examined.

2. The bridge

2.1. The Free Vibrating Bridge

The complete equation of Timoshenko beam is given by

$$EJ_y \frac{\partial^4 w}{\partial x^4} + m\cdot\frac{\partial^2 w}{\partial t^2} - \left(\frac{EJ_y m}{k'AG} + \rho J_y\right)\cdot\frac{\partial^4 w}{\partial^2 x \partial^2 t} + \frac{\rho J_y m}{k'AG}\cdot\frac{\partial^4 w}{\partial t^4} = p + \frac{\rho J_y}{k'AG}\ddot{p} - \frac{EJ_y}{k'AG}p'' \qquad (1)$$

From (1) ignoring the term $\frac{\rho m}{k'AG}\cdot\frac{\partial^4 w}{\partial t^4}$ as very small, the following equation of the free vibrating bridge is obtained by

$$\frac{\partial^4 w}{\partial x^4} + \frac{m}{EJ_y}\cdot\frac{\partial^2 w}{\partial t^2} - \left(\frac{m}{k'AG} + \frac{\rho}{E}\right)\cdot\frac{\partial^4 w}{\partial^2 x \partial^2 t} + \frac{\rho m}{k'AGE}\cdot\frac{\partial^4 w}{\partial t^4} = 0 \qquad (2)$$

According to [1], from equation (2) we get the following expressions for the eigenfrequencies and shape functions of a simply supported one-span bridge of length L

$$\left.\begin{aligned} \omega_n^2 &= \frac{n^4\pi^4}{L^2}\cdot\frac{\upsilon_M^2\upsilon_Q^2}{(n^2\pi^2+\lambda^2)\upsilon_Q^2 + n^2\pi^2\upsilon_M^2} \\ X_n(x) &= \sin\frac{n\pi x}{L} \end{aligned}\right\} \qquad (3)$$

where $\upsilon_M = \sqrt{E/\rho}$, $\upsilon_Q = \sqrt{k'G/\rho}$ are the moment and the shear wave velocities respectively and λ is the slenderness of the bridge.

2.2. The Forced Vibrating Bridge

Neglecting in Eq(1), as very small, the terms containing the factors $m\rho I_y / k'AG$ and $\rho I_y / k'AG$, and taking into account the bridge's damping, the equation of forced vibration becomes

$$EJ_y \frac{\partial^4 w}{\partial x^4} + c\frac{\partial w}{\partial t} + m\cdot\frac{\partial^2 w}{\partial t^2} - \left(\frac{EJ_y m}{k'AG} + \rho J_y\right)\cdot\frac{\partial^4 w}{\partial^2 x \partial^2 t} = p - \frac{EJ_y}{k'AG}p'' \qquad \text{or}$$

$$w''''(x,t) + \frac{c}{EI_y}\dot{w}(x,t) + \frac{m}{EI_y}\ddot{w}(x,t) - \left(\frac{m}{k'AG} + \frac{\rho}{E}\right)\cdot\ddot{w}''(x,t) = \frac{p(x,t)}{EI_y} - \frac{1}{k'AG}p''(x,t) \qquad (4)$$

We are searching for a solution of the form

$$w(x,t) = \sum_n X_n(x)\; T_n(t) \qquad (5)$$

where $X_n(x)$ represent the shape functions of the bridge and $T_n(t)$ the unknown time functions under determination. For the one span beam, X_n is given by Eq (3b).

Eq (4), because of Eq (5), becomes

$$\begin{aligned}\sum_n \frac{n^4\pi^4}{L^4}\cdot \sin\frac{n\pi x}{L}\cdot T_n + \frac{c}{EI_y}\sum_n \sin\frac{n\pi x}{L}\cdot\dot{T}_n + \frac{m}{EI_y}\sum_n \sin\frac{n\pi x}{L}\cdot\ddot{T}_n \\ +\left(\frac{\rho}{k'G} + \frac{\rho}{E}\right)\sum_n \frac{n^2\pi^2}{L^2}\sin\frac{n\pi x}{L}\cdot\ddot{T}_n = \frac{p(x,t)}{EI_y} - \frac{1}{k'AG}p''(x,t)\end{aligned} \qquad (6a)$$

Multiplying last eq. by $\sin\frac{n\pi x}{L}$, integrating from 0 to L and taking into account the orthogonality condition, Eq(6a) results to

$$\frac{L}{2}\cdot\left\{\frac{n^4\pi^4}{L^4}T_n + \frac{c}{EI_y}\dot{T}_n + \left[\frac{m}{EI_y} + \frac{n^2\pi^2}{L^2}\left(\frac{1}{\upsilon_M^2} + \frac{1}{\upsilon_Q^2}\right)\right]\ddot{T}_n\right\} = \frac{\int_0^L p\sin\frac{n\pi x}{L}dx}{EI_y} - \frac{\int_0^L p''\sin\frac{n\pi x}{L}dx}{k'AG} \qquad (6b)$$

The Using of the following expressions which are valid:

$$\left.\begin{aligned}
&\frac{m}{EI_y} = \frac{\rho A}{EI_y} = \frac{1}{\upsilon_M^2} + \frac{1}{r_y^2} = \frac{\lambda^2}{L^2\,\upsilon_M^2}\\
&\frac{c}{EI_y} = \frac{c}{m}\cdot\frac{m}{EI_y} = \frac{c}{m}\cdot\frac{\lambda^2}{L^2\,\upsilon_M^2}\\
&\frac{m}{k'AG} + \frac{\rho}{E} = \frac{\rho A}{k'AG} + \frac{\rho}{E} = \frac{1}{\upsilon_M^2} + \frac{1}{\upsilon_Q^2}\\
&\frac{1}{EI_y} = \frac{1}{m}\cdot\frac{m}{EI_y} = \frac{\lambda^2}{m\,L^2\,\upsilon_M^2}\\
&\frac{1}{k'AG} = \frac{1}{m}\cdot\frac{m}{k'AG} = \frac{1}{m\,\upsilon_Q^2}\\
&\frac{m}{EI_y} + \frac{n^2\pi^2}{L^2}\left(\frac{1}{\upsilon_M^2} + \frac{1}{\upsilon_Q^2}\right) = \frac{\lambda^2}{L^2\,\upsilon_M^2} + \frac{n^2\pi^2}{L^2}\cdot\frac{\upsilon_M^2 + \upsilon_Q^2}{\upsilon_M^2\cdot\upsilon_Q^2} = \frac{1}{L^2}\cdot\frac{(n^2\pi^2 + \lambda^2)\upsilon_Q^2 + n^2\pi^2\upsilon_M^2}{\upsilon_M^2\cdot\upsilon_Q^2}
\end{aligned}\right\} \qquad (6c)$$

Leads to

$$\left.\begin{aligned}
&\frac{n^4\pi^4}{L^4}\cdot L^2\cdot\frac{\upsilon_M^2\cdot\upsilon_Q^2}{(n^2\pi^2+\lambda^2)\upsilon_Q^2+n^2\pi^2\upsilon_M^2}=\frac{n^4\pi^4}{L^2}\cdot\frac{\upsilon_M^2\cdot\upsilon_Q^2}{(n^2\pi^2+\lambda^2)\upsilon_Q^2+n^2\pi^2\upsilon_M^2}=\omega_n^2\\
&\frac{c}{EI_y}\cdot L^2\cdot\frac{\upsilon_M^2\cdot\upsilon_Q^2}{(n^2\pi^2+\lambda^2)\upsilon_Q^2+n^2\pi^2\upsilon_M^2}=\frac{c}{m}\cdot\frac{\lambda^2}{L^2\upsilon_M^2}\cdot L^2\cdot\frac{\upsilon_M^2\cdot\upsilon_Q^2}{(n^2\pi^2+\lambda^2)\upsilon_Q^2+n^2\pi^2\upsilon_M^2}=\\
&\qquad\qquad=\frac{c}{m}\cdot\frac{\lambda^2\cdot\upsilon_Q^2}{(n^2\pi^2+\lambda^2)\upsilon_Q^2+n^2\pi^2\upsilon_M^2}\\
&\frac{1}{EI_y}\cdot L^2\cdot\frac{\upsilon_M^2\cdot\upsilon_Q^2}{(n^2\pi^2+\lambda^2)\upsilon_Q^2+n^2\pi^2\upsilon_M^2}\cdot\frac{2}{L}=\frac{\lambda^2}{mL^2\upsilon_M^2}\cdot L^2\cdot\frac{\upsilon_M^2\cdot\upsilon_Q^2}{(n^2\pi^2+\lambda^2)\upsilon_Q^2+n^2\pi^2\upsilon_M^2}\cdot\frac{2}{L}=\\
&\qquad\qquad=\frac{2}{mL}\cdot\frac{\lambda^2\cdot\upsilon_Q^2}{(n^2\pi^2+\lambda^2)\upsilon_Q^2+n^2\pi^2\upsilon_M^2}\\
&\frac{1}{k'AG}\cdot L^2\cdot\frac{\upsilon_M^2\cdot\upsilon_Q^2}{(n^2\pi^2+\lambda^2)\upsilon_Q^2+n^2\pi^2\upsilon_M^2}\cdot\frac{2}{L}=\frac{1}{m\upsilon_Q^2}\cdot L^2\cdot\frac{\upsilon_M^2\cdot\upsilon_Q^2}{(n^2\pi^2+\lambda^2)\upsilon_Q^2+n^2\pi^2\upsilon_M^2}\cdot\frac{2}{L}=\\
&\qquad\qquad=\frac{2L}{m}\cdot\frac{\upsilon_M^2}{(n^2\pi^2+\lambda^2)\upsilon_Q^2+n^2\pi^2\upsilon_M^2}
\end{aligned}\right\}\tag{6d}$$

Therefore, equation (6b) becomes

$$\left.\ddot{T}_n+2\beta_n\dot{T}_n+\omega_n^2T_n=A_n\int_0^L p\sin\frac{n\pi x}{L}dx-B_n\int_0^L p''\sin\frac{n\pi x}{L}dx\right\}\tag{7}$$

$$\left.\begin{aligned}
\text{where:}\quad 2\beta_n&=\frac{c}{m}\cdot\frac{\lambda^2\cdot\upsilon_Q^2}{(n^2\pi^2+\lambda^2)\upsilon_Q^2+n^2\pi^2\upsilon_M^2}\\
A_n&=\frac{2}{mL}\cdot\frac{\lambda^2\cdot\upsilon_Q^2}{(n^2\pi^2+\lambda^2)\upsilon_Q^2+n^2\pi^2\upsilon_M^2}\\
B_n&=\frac{2}{mL}\cdot\frac{L^2\upsilon_M^2}{(n^2\pi^2+\lambda^2)\upsilon_Q^2+n^2\pi^2\upsilon_M^2}
\end{aligned}\right\}\tag{8}$$

and ω_n from equation (3a).

The solution of equation (7), is given by Duhamel's integral as follows.

$$\left.\begin{aligned}
&T_n(t)=\frac{1}{\overline{\omega}_n}\cdot\int_0^t\left(A_n\int_0^L p(x,\tau)\sin\frac{n\pi x}{L}dx-B_n\int_0^L p''(x,\tau)\sin\frac{n\pi x}{L}dx\right)e^{-\beta(t-\tau)}\sin\overline{\omega}_n(t-\tau)d\tau\\
&\text{where:}\quad \overline{\omega}_n^2=\omega_n^2-\beta^2
\end{aligned}\right\}\tag{9}$$

3. Finite Beam on Elastic Foundation

Let us consider now beam AB of figure 1, which is based on an elastic foundation of Winkler type. According to classic theory, the force per unit length of the beam reacting to the external loading is

$$\left.P=k\cdot w\right\}\tag{10}$$

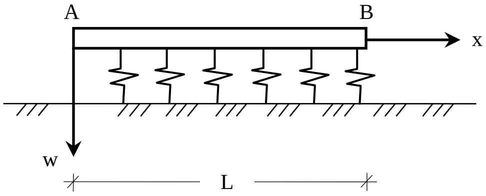

Figure 1. Finite beam on elastic foundation.

where k is the so-called Winkler factor. Let us determine this factor.

It has been experimentally proven that the pressure σ_z under a foundation of square surface in relation to the depth z, is given by the curve of figure 2 [38].

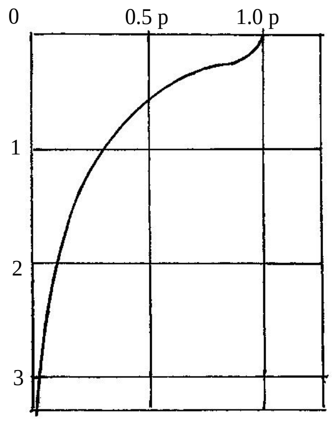

Figure 2. σ_z in relation to the depth z (experimental curve).

From this diagram, we observe that the pressure σ_z for depth greater than 3.5 meters is practically equal to zero.

There are many studies that try to determine an algebraic expression of Winkler's factor k. A list of these efforts can be found in [39].

Since the present study has no geotechnical ambitions but only aims to use a qualitative expression of factor k, we will use the rather simple expression given by Vesic [40].

In [34], Vesic tried to develop a formula giving k, where instead of equating bending moments, he equated the maximum displacements of the beam. Vesic concluded to the following empirical formula giving k:

$$k = \frac{0.65 \cdot E_s}{1-\nu_s^2} \cdot \left(\frac{b^4 E_s}{E I_y} \right)^{0.0833} \quad (11)$$

where E_s is the modulus of elasticity of the soil, ν_s is the Poisson's ratio of the soil, b is the beam width, and EI_y is the bending rigidity of the beam.

3.1. The Free Vibrating Beam

Introducing the reaction of foundation into equation (1) we get:

$$E J_y \frac{\partial^4 w}{\partial x^4} + m \frac{\partial^2 w}{\partial t^2} - \left(\frac{EJ_y m}{k'AG} + \rho J_y \right) \frac{\partial^4 w}{\partial^2 x \partial^2 t} + k \cdot w = p \quad (12)$$

where the terms of higher order have been neglected.
The equation of free vibrating beam is:

$$\frac{\partial^4 w}{\partial x^4} + \frac{m}{EJ_y} \frac{\partial^2 w}{\partial t^2} - \left(\frac{m}{k'AG} + \frac{\rho}{E} \right) \frac{\partial^4 w}{\partial^2 x \partial^2 t} + \frac{k}{EJ_y} w = 0 \quad (13)$$

Following a procedure similar to the one of section 3 and considering boundary conditions which prevent the subsidence of beam's edges, we conclude to the following relations giving the eigenfrequencies and shape functions [1]:

$$\left.\begin{aligned} &\omega_n^2 = \left(\frac{n^4\pi^4}{L^2} + \frac{k\lambda^2}{m\upsilon_M^2}\right)\cdot\frac{\upsilon_M^2\,\upsilon_Q^2}{(n^2\pi^2+\lambda^2)\upsilon_Q^2 + n^2\pi^2\upsilon_M^2} \\ &X_n(x) = \sin\frac{n\pi x}{L} \end{aligned}\right\} \tag{14}$$

3.2. The Forced Vibrating Beam

Neglecting in Eq(1), as very small, the terms containing the factors $m\rho I_y / k'AG$ and $\rho I_y / k'AG$, and taking into account the beam's damping and the reaction of foundation, the equation of forced vibration becomes:

$$EJ_y\frac{\partial^4 w}{\partial x^4} + c\frac{\partial w}{\partial t} + m\cdot\frac{\partial^2 w}{\partial t^2} - \left(\frac{EJ_y m}{k'AG} + \rho J_y\right)\cdot\frac{\partial^4 w}{\partial^2 x\partial^2 t} + k\cdot w = p - \frac{EJ_y}{k'AG}p'' \qquad \text{or}$$

$$\left.\begin{aligned} &w''''(x,t) + \frac{c}{EI_y}\dot{w}(x,t) + \frac{m}{EI_y}\ddot{w}(x,t) - \left(\frac{m}{k'AG} + \frac{\rho}{E}\right)\cdot\ddot{w}''(x,t) + \frac{k}{EI_y}\cdot w(x,t) \\ &\qquad = \frac{p(x,t)}{EI_y} - \frac{1}{k'AG}p''(x,t) \end{aligned}\right\} \tag{15}$$

We are searching for a solution of the form

$$w(x,t) = \sum_n X_n(x)\, T_n(t) \tag{16}$$

where $X_n(x)$ represent the shape functions of the bridge and $T_n(t)$ the unknown time functions which are under determination. For one span beam, X_n is given by Eq (14b).
Using Eq (14) and (16), Eq (15) becomes:

$$\left.\begin{aligned} &\sum_n\left(\frac{n^4\pi^4}{L^4} + \frac{k}{EI_y}\right)\cdot\sin\frac{n\pi x}{L}\cdot T_n + \frac{c}{EI_y}\sum_n \sin\frac{n\pi x}{L}\cdot\dot{T}_n + \frac{m}{EI_y}\sum_n \sin\frac{n\pi x}{L}\cdot\ddot{T}_n \\ &\qquad + \left(\frac{m}{k'AG} + \frac{\rho}{E}\right)\sum_n\frac{n^2\pi^2}{L^2}\sin\frac{n\pi x}{L}\cdot\ddot{T}_n = \frac{p(x,t)}{EI_y} - \frac{1}{k'AG}p''(x,t) \end{aligned}\right\} \tag{17}$$

Multiplying last equation by $\sin\frac{n\pi x}{L}$, integrating from 0 to L and taking into account the orthogonality condition, equation (17) becomes

$$\frac{L}{2}\cdot\left\{\left(\frac{n^4\pi^4}{L^4} + \frac{k}{EI_y}\right)T_n + \frac{c}{EI_y}\dot{T}_n + \left[\frac{m}{EI_y} + \frac{n^2\pi^2}{L^2}\left(\frac{1}{\upsilon_M^2} + \frac{1}{\upsilon_Q^2}\right)\right]\ddot{T}_n\right\} = \frac{\int_0^L p\sin\frac{n\pi x}{L}dx}{EI_y} - \frac{\int_0^L p''\sin\frac{n\pi x}{L}dx}{k'AG} \tag{18}$$

The above, because of the expressions (6c) and (6d), becomes

$$\ddot{T}_n + 2\beta_n\dot{T}_n + \omega_n^2 T_n = A_n\int_0^L p\sin\frac{n\pi x}{L}dx - B_n\int_0^L p''\sin\frac{n\pi x}{L}dx \tag{19}$$

where β_n, A_n, B_n given by equation (8) and

$$\omega_n = \sqrt{\left(\frac{n^4\pi^4}{L^2} + \frac{k\lambda^2}{m\upsilon_M^2}\right)\cdot\frac{\upsilon_M^2\,\upsilon_Q^2}{(n^2\pi^2+\lambda^2)\upsilon_Q^2 + n^2\pi^2\upsilon_M^2}} \tag{20}$$

The solution of (19) is given by Duhamel's integral of equation (9).

4. Numerical Results and Discussion

Two are the main materials used in bridge engineering which are Steel and Concrete and the main used cross-sections for decks are the orthogonal, the I open sections and the box (closed) cross-sections. The materials, cross-sections' data, the resulting Timoshenko's coefficients and wave propagation speeds are shown in the following Table 1.

Table 1. Speeds of moment and shear waves for various types of cross sections.

Material	E dN/m^2	G dN/m^2	Poisson ratio ν	ρ kg/m^3	Cross-section	k’	υ_M m/sec	υ_Q m/sec
Steel	2.1×10^{10}	0.8×10^{10}	0.30	800		0.46	5150	2144
						0.65	5150	2550
Concrete	0.35×10^{10}	0.01×10^{10} to 0.20×10^{10}	0.20	240		0.83	3818	588 to 2630
						0.46	3818	438 to 1957
						0.65	3818	540 to 2327

Let us consider now a simply supported bridge made of steel or concrete with length L ranging from 20 to 80 meters. The other data of the bridge is shown in the following table 2.

Table 2. Shear Timoshenko coefficient and slenderness ratio for various lengths and cross-sections of the beam.

Material	k'	υ_M	υ_Q	L	I_y	A	m	λ
Steel	0.46	5150	2144	80	7.8	1.27	1000	30
				60	2.22	0.77	600	36
				40	0.06	0.51	400	97
	0.65	5150	2550	80	7.8	1.27	1000	30
				60	2.22	0.77	600	36
				40	0.06	0.51	400	97
Concrete	0.83	3820	588 to 2630	40	1.0	2.90	700	69
				20	0.08	1.25	300	91
	0.46	3820	438 to 1957	60	1.50	2.50	600	80
				40	1.25	2.00	480	50
				20	0.45	1.00	240	30
	0.65	3820	540 to 2327	60	1.50	2.50	600	80
				40	1.25	2.00	480	50
				20	0.45	1.00	240	30

For a beam on elastic foundation we have chosen a concrete beam, having orthogonal cross-section with characteristics shown in Table 1 (line 4) and Table 2 (lines 7 and 8).

Table 3. Soil characteristics.

SOIL	E_s dN/cm^2	ν_s
Sand	500 – 800	0.15 – 0.4
Dense sand	160 – 500	0.15
Argil sand	100 – 200	0.15
Mortal	15 – 150	0.3 – 0.35
Thin argil	15 – 150	0.1 – 0.3
Fat argil	15 – 150	0.1 – 0.3
Turf	1 – 5	0.3 – 0.4
Organic clays	0.5 - 4	0.4 – 0.5

Soil characteristics of different grades are given in the following table 3.

The bridges and beams considered are subject to loads, moving with speeds v=105 km/h (speed of usual trains), v=300 km/h (fast trains) and v=540km/h (super fast trains).

4.1. Bridge of Steel Under Moving Loads

Applying the formulae of section 2 we obtain the following plots (figures 3 to 8) for steel bridges with open or closed (box) cross-sections and lengths L=80, 60, and 40 meters.

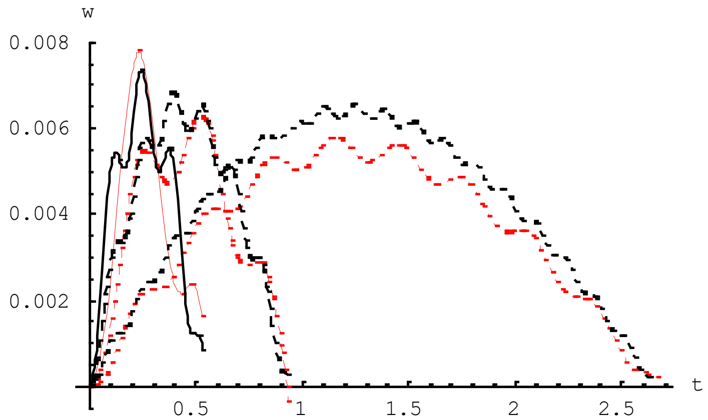

Figure 3. The deformation w (meters) of the middle of the bridge relating to time t (seconds), according to the improved formulae (red) and to the classical ones (black) for open cross-section, length L=80mand various speeds: (. . . .) 105 km/h, (- - -) 300km/h, (____) 540 km/h.

From the above plot of figure 3, it can easily be seen that, for speeds 105 and 300 km/h, the improved formulae give smaller deformations than the classic ones, but for super fast speeds happens the opposite. The difference for the speed of 105 km/h amounts to about -12%, for the speed of 300 km/h amounts to about -8%, while for the speed of 540 km/h amounts to about +7.5%.

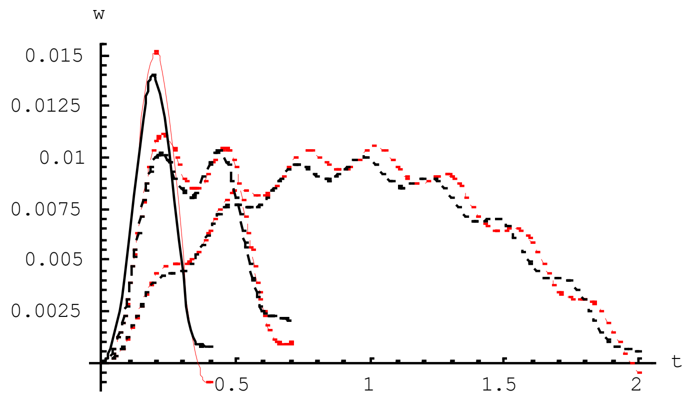

Figure 4. The deformation w (meters) of the middle of the bridge relating to time t (seconds), according to the improved formulae (red) and to the classical ones (black) for open cross-section, length L=60mand various speeds: (. . . .) 105 km/h, (- - -) 300km/h, (____) 540 km/h.

From the above plot of figure 4, it can easily be seen that the improved formulae give greater deformations than the classic ones for any speed. The difference for the speed of 105 km/h amounts to about +5%, for the speed of 300 km/h amounts to about +1.5% while for the speed of 540 km/h amounts to about +4.5%.

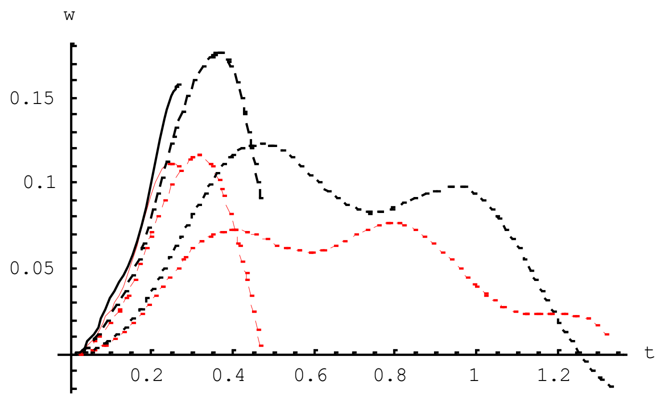

Figure 5. The deformation w (meters) of the middle of the bridge relating to time t (seconds), according to the improved formulae (red) and to the classical ones (black) for open cross-section, length L=40mand various speeds: (. . . .) 105 km/h, (- - -) 300km/h, (____) 540 km/h.

From the above plot of figure 5, it can easily be seen that the improved formulae give smaller deformations than the classic ones for any speed. The difference for the speed of 105 km/h amounts to about -35%, for the speed of 300 km/h amounts to about -30% and for the speed of 540 km/h amounts to about -27%.

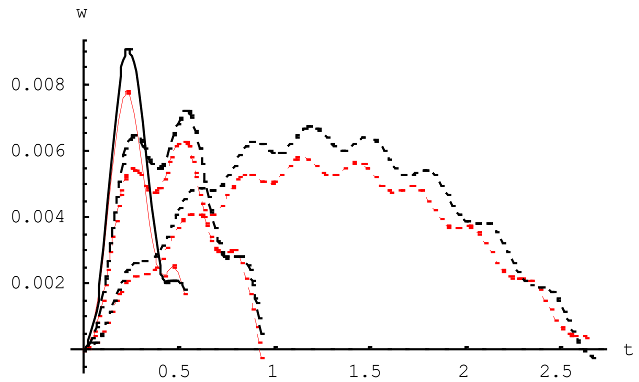

Figure 6: The deformation w (meters) of the middle of the bridge relating to time t (seconds), according to the improved formulae (red) and to the classical ones (black) for open cross-section, length L=80mand various speeds: (. . . .) 105 km/h, (- - -) 300km/h, (____) 540 km/h.

From the above plot of figure 6, it can easily be seen that the improved formulae give smaller deformations than the classic ones for any speed. The difference for the speed of 105 km/h amounts to about -15%, for the speed of 300 km/h amounts to about -12% while for the speed of 540 km/h amounts to about -15%.

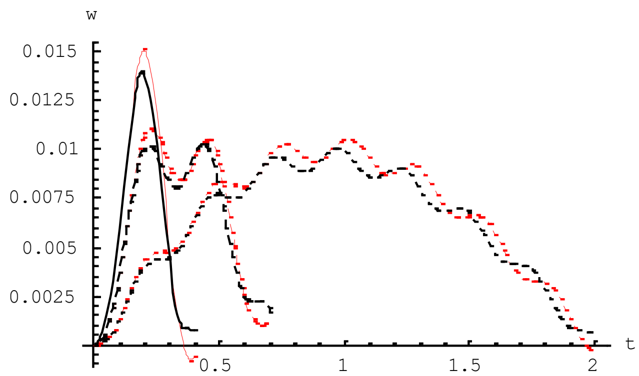

Figure 7. The deformation w (meters) of the middle of the bridge relating to time t (seconds), according to the improved formulae (red) and to the classical ones (black) for open cross-section, length L=60mand various speeds: (. . . .) 105 km/h, (- - -) 300km/h, (____) 540 km/h.

From the above plot of figure 7, it can easily be seen that the improved formulae give greater deformations than the classic ones for any speed. The difference for the speed of 105 km/h amounts to about +6%, for the speed of 300 km/h amounts to about +3% while for the speed of 540 km/h amounts to about +7%.

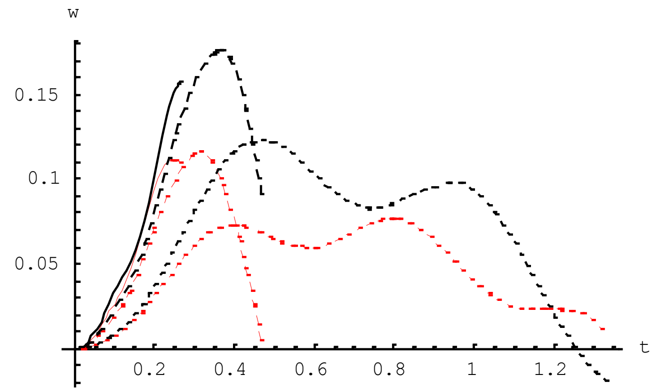

Figure 8. The deformation w (meters) of the middle of the bridge relating to time t (seconds), according to the improved formulae (red) and to the classical ones (black) for open cross-section, length L=40mand various speeds: (. . . .) 105 km/h, (- - -) 300km/h, (____) 540 km/h.

From the above plot of figure 8, it can easily be seen that the improved formulae give smaller deformations than the classic ones for any speed. The difference for the speed of 105 km/h amounts to about -38%, for the speed of 300 km/h amounts to about -35% and for the speed of 540 km/h amounts to about -30%.

4.2. Bridge of Concrete Under Moving Loads

Applying the formulae of section 2 we obtain the following plots of figures 9 to 14 for concrete bridges with open or closed (box) cross-sections and lengths L=60, 40, and 20 meters.

The differences between concrete bridges with open and closed cross-sections but with the same υ_Q are negligible (<0.3%), while the differences become noticeable for different υ_Q (different concrete quality), as it can be seen in the diagrams of figures 9 to 14.

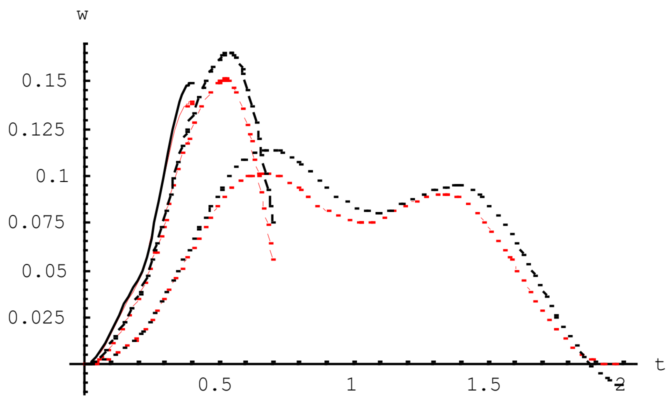

Figure 9. The deformation w (meters) of the middle of the bridge relating to time t (seconds), according to the improved formulae (red) and to the classical ones (black) for open or box cross-section, length L=60m,υ_Q =1900 and various speeds: (. . . .) 105 km/h, (- - -) 300km/h, (____) 540 km/h.

From the above plot of figure 9, we can easily see that the improved formulae give smaller deformations than the classic ones for any speed. The difference for the speed of 105 km/h amounts to about -10%, for the speed of 300 km/h amounts to about -18% and for the speed of 540 km/h amounts to about -16%.

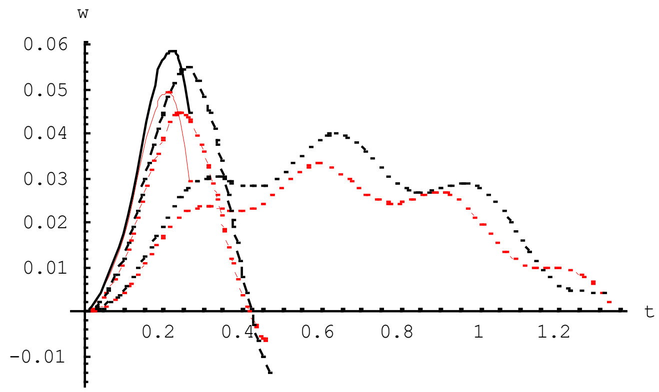

Figure 10. The deformation w (meters) of the middle of the bridge relating to time t (seconds), according to the improved formulae (red) and to the classical ones (black) for open or box cross-section, length L=40m,υ_Q =1900 and various speeds: (. . . .) 105 km/h, (- - -) 300km/h, (____) 540 km/h.

From the above plot of figure 10, we can easily see that the improved formulae give smaller deformations than the classic ones for any speed. The difference for the speed of 105 km/h amounts to about -15%, for the speed of 300 km/h amounts to about -17% and for the speed of 540 km/h amounts to about -20%.

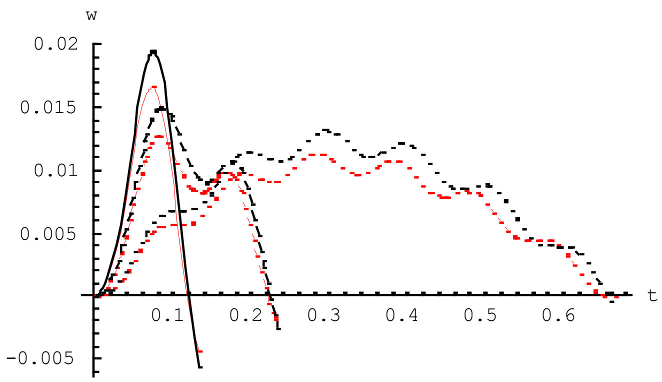

Figure 11. The deformation w (meters) of the middle of the bridge relating to time t (seconds), according to the improved formulae (red) and to the classical ones (black) for open or box cross-section, length L=20m,υ_Q =1900 and various speeds: (. . . .) 105 km/h, (- - -) 300km/h, (____) 540 km/h.

From the above plot of figure 11, we can easily see that the improved formulae give smaller deformations than the classic ones for any speed. The difference for the speed of 105 km/h amounts to about -13%, for the speed of 300 km/h amounts to about -14% and for the speed of 540 km/h amounts to about -14%.

From the plot of figure 12, we can easily see that the improved formulae give smaller deformations than the classic ones for any speed. The difference for the speed of 105 km/h amounts to about -3%, for the speed of 300 km/h amounts to about -9% and for the speed of 540 km/h amounts to about -5%.

From the plot of figure 13, we can easily see that the improved formulae give smaller deformations than the classic ones for any speed. The difference for the speed of 105 km/h amounts to about -15%, for the speed of 300 km/h amounts to about -17% and for the speed of 540 km/h amounts to about -15%.

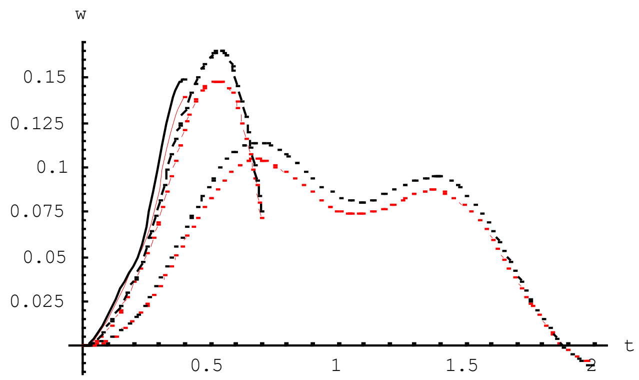

Figure 12. The deformation w (meters) of the middle of the bridge relating to time t (seconds), according to the improved formulae (red) and to the classical ones (black) for open or box cross-section, length L=60m,υ_Q =500 and various speeds: (. . . .) 105 km/h, (- - -) 300km/h, (____) 540 km/h.

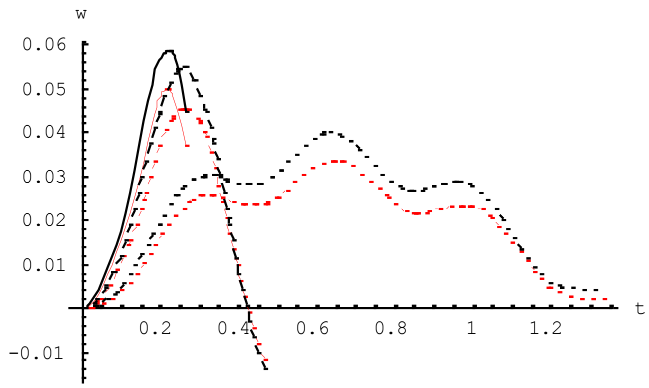

Figure 13. The deformation w (meters) of the middle of the bridge relating to time t (seconds), according to the improved formulae (red) and to the classical ones (black) for open or box cross-section, length L=40m,υ_Q =500 and various speeds: (. . . .) 105 km/h, (- - -) 300km/h, (____) 540 km/h.

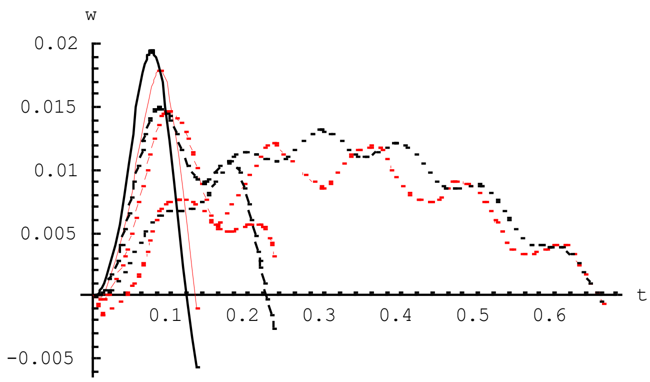

Figure 14. The deformation w (meters) of the middle of the bridge relating to time t (seconds), according to the improved formulae (red) and to the classical ones (black) for open or box cross-section, length L=20m,υ_Q =500 and various speeds: (. . . .) 105 km/h, (- - -) 300km/h, (____) 540 km/h.

From the above plot of figure 14, we can easily see that the improved formulae give smaller deformations than the classic ones for any speed. The difference for the speed of 105 km/h amounts to about -8%, for the speed of 300 km/h amounts to about -6% and for the speed of 540 km/h amounts to about -8%.

4.3. Beam on Elastic Foundation

Applying the data in Table 3 and according to the formulae of section 4 one can see that the coefficient k of Winkler ranges from 0.222×10^4 to 5.64×10^6.

Applying the formulae of section 3, we obtain the following plots of figures 15 to 18 for a beam (of dimensions b = 2m, and h = 0.5m), on elastic foundation of thickness H = 2m, for soil of mortal with $E_s = 50$ dn/cm^2, $\nu_s = 0.15$ and $\rho_s = 190$ kg/m^3 and $k = 0.279\times10^6$.

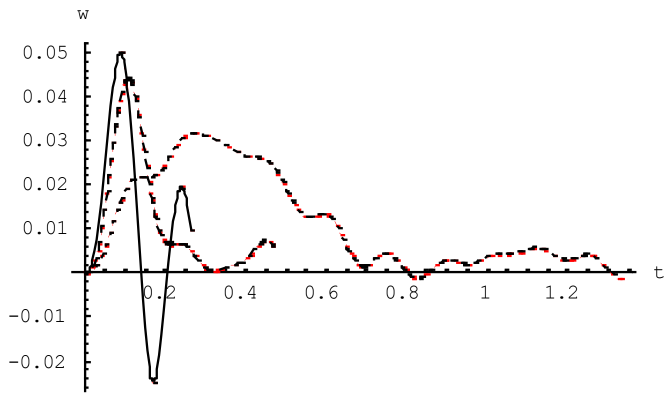

Figure 15. The deformation w (meters) of the middle of the beam relating to time t (seconds), according to the improved formulae (red) and to the classical ones (black) for rectangular cross-section, length L=40m, λ=277, υ_Q =1900 and various speeds: (. . . .) 105 km/h, (- - -) 300km/h, (____) 540 km/h.

From the above plot of figure 15, we see that the improved formulae give greater deformations than the classic ones for any speed. The difference for the speed of 105 km/h amounts to about +0.35%, for the speed of 300 km/h amounts to about +0.34% and for the speed of 540 km/h amounts to about +0.32%.

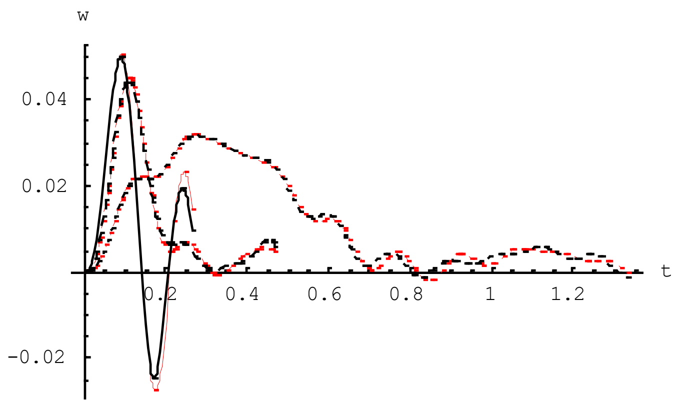

Figure 16. The deformation w (meters) of the middle of the beam relating to time t (seconds), according to the improved formulae (red) and to the classical ones (black) for rectangular cross-section, length L=40m λ=277, υ_Q =500 and various speeds: (. . . .) 105 km/h, (- - -) 300km/h, (____) 540 km/h.

From the above plot of figure 16, we see that the improved formulae give greater deformations than the classic ones for any speed. The difference for the speed of 105 km/h amounts to about 0%, for the speed of 300 km/h amounts to about +0.01% and for the speed of 540 km/h amounts to about +0.012%.

From the plot of figure 17, we see that the improved formulae give greater deformations than the classic ones for any speed. The difference for the speed of 105 km/h amounts to about -0.01%, for the speed of 300 km/h amounts to about ~0% and for the speed of 540 km/h amounts to about +0.03%.

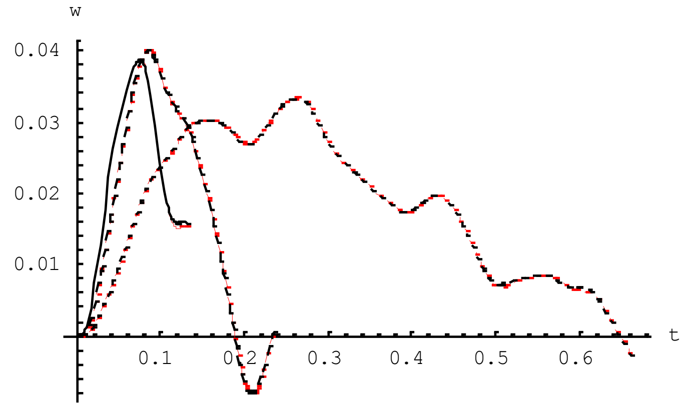

Figure 17. The deformation w (meters) of the middle of the beam relating to time t (seconds), according to the improved formulae (red) and to the classical ones (black) for rectangular cross-section, length L=40m υ_Q =500 and various speeds: (. . . .) 105 km/h, (- - -) 300km/h, (____) 540 km/h.

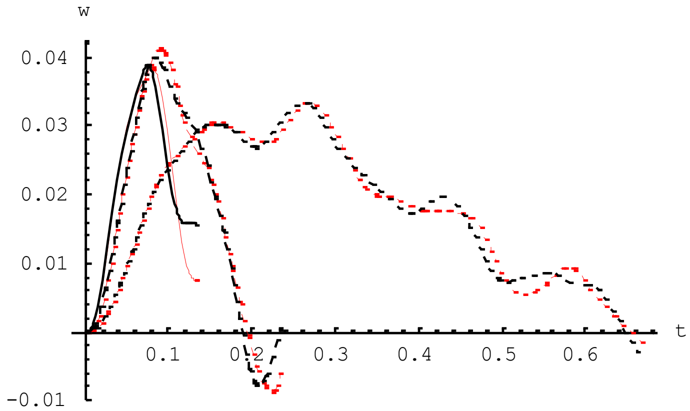

Figure 18. The deformation w (meters) of the middle of the beam relating to time t (seconds), according to the improved formulae (red) and to the classical ones (black) for rectangular cross-section, length L=20m υ_Q =500 and various speeds: (. . . .) 105 km/h, (- - -) 300km/h, (____) 540 km/h.

From the above plot of figure 18, we see that the improved formulae give greater deformations than the classic ones for any speed. The difference for the speed of 105 km/h amounts to about -1.2%, for the speed of 300 km/h amounts to about +3.6% and for the speed of 540 km/h amounts to about +1.3%.

5. Conclusions

From the diagrams and plots of section 4, we conclude the following.

5.1. Dynamic Behavior of Bridges

a) For steel bridges using the exact theory we have the following differences on deformations compared to the ones got by the classic theory:

For L = 80m, speed 105 km/h, open cross-section +12%, box cross-section -15%

	“	300	“	“	“	“	- 8%,	“	“	“	-12%
	“	540	“	“	“	“	- 7.5%,	“	“	“	-15%
For L = 40m,	“	105	“	“	“	“	+ 5%,	“	“	“	+ 6%
	“	300	“	“	“	“	+ 1.5%	“	“	“	+3%
	“	540	“	“	“	“	+ 4.5%	“	“	“	+7%
For L = 20m	“	105	“	“	“	“	- 35%	“	“	“	-38%
	“	300	“	“	“	“	- 30%	“	“	“	-35%
	“	540	“	“	“	“	- 27%	“	“	“	-30%

b) For bridges made from concrete the differences depend both on the concrete quality and also on whether it is cracked or not.

Both of the above factors can be expressed by the velocity υ_Q.

For concrete bridges using the exact theory we have the following differences on deformations compared to the ones got by the classic theory:

For L = 60m,	speed 105	km/h,	open or box cross-section,	υ_Q=1900	-10%,	υ_Q=500	-3%
	“ 300	“	“ “ “ “	“ “	-18%	“	-9%
	“ 540	“	“ “ “ “	“ “	-16%	“	-5%
For L = 40m,	“ 105	“	“ “ “ “	“ “	-15%	“	-15%
	“ 300	“	“ “ “ “	“ “	-17%	“	-17%
	“ 540	“	“ “ “ “	“ “	-20%	“	-15%
For L = 20m,	“ 105	“	“ “ “ “	“ “	-13%	“	-8%
	“ 300	“	“ “ “ “	“ “	-14%	“	-6%
	“ 540	“	“ “ “ “	“ “	-14%	“	-8%

5.2. Dynamic Behavior of a Beam on Elastic Foundation

The observed differences between the exact and the classic theory are negligible ranging from 0 to -0.5% and they are reduced for foundations on more compact soils.

It would be of great interest to continue the above study for concrete bridge in relation with the quality of concrete and if it is cracked or not.

References

[1] T. G. Konstantakopoulos, I. G. Raftoyiannis and G. T. Michaltsos, The influence of traveling waves on eigen frequencies and critical speeds of a beam”, The open Mechanics Journal, vol 3, pp.12-19, 2009.

[2] M. Redwood, Mechanical Wave guides, Pergamon Press, New York, 1960.

[3] Y. K. Chenny, Finite strip method in Structural Analysis, Pergamon Press, New York, 1997.

[4] F. K. Graff, Wave motion in Elastic Solids, Dover Publ. Inc., New York, 1991.

[5] L. Treloar, The Physics of Rubber Elasticity, Clarendon Press, Oxford, UK, 1975.

[6] N. Muskhilishvili, Some Basic Problem of the Mathematical Theory of Elasticity, Noordhoff, Leiden, The Netherlands, 1975.

[7] J. Allard, Propagation of Sound in Porous Media, Elsevier Science, Essex, UK, 1993.

[8] H. Zhao and G. Gary, A three dimensional analytical solution of the longitudinal wave propagation in an infinite linear viscoelastic cylindrical bar. Application to experimental techniques, Journal of the Mechanics and Physics of Solids, vol 43(8), pp. 1335-1348, 1995.

[9] A. D. Drozdov and A. Dorfmann, The nonlinear viscoelastic response of carbon black-filled natural rubbers, Int. Journal of Solids and Structures, vol 39(23), pp. 5699-5717, 2002.

[10] A. Betaner, D. Rittel, and A. L. Yarin, Theoretical and experimental analysis of longitudinal wave propagation in cylindrical viscoelastic rods, Journal of the Mechanics and Physics of Solids, vol 51(8), pp. 1413-1431, 2003.

[11] E. Manconi and B. R. Mace, Wave characterization of cylindrical and curved panels using a finite element method, Journal of the Acoustic Society of America, vol 125, pp. 154-163, 2009.

[12] K. J. Bathe, Finite Element Procedures in Engineering Analysis, Prentice-Hall, Englewood Cliffs, 1982.

[13] J. M. Renno, E. Manconi and B. R. Mace, A Finite Element Method for Modelling Waves in

Laminated Structures, Advances in Structural Engineering, vol 16, pp. 61-75, 2013.

[14] B. R. Mace and E. Manconi, Modelling wave propagation in two-dimensional structures using finite element analysis, Journal of Sound and Vibration, vol 318, pp. 884-902, 2008.

[15] S. Corn, N. Bouhaddi and J. Piranda, Transverse Vibrations of Short Beams: Finite Element Models Obtained by a Condensation Method, J. of Sound and Vibration, vol 201(3), pp. 353-363, 1997.

[16] F. Montiel, V. A. Squire and L. G. Bennets, Evolution of directional spectra through finite regular and randomly perturbed arrays of scatterers, Siam J. of Appl. Math., vol 75, pp. 630-651, 2015.

[17] J. F. Doyle, Aspectrally formulation finite element for longitudinal wave propagation, Int. Journal of Analytical and Experimental Modal analysis, vol (3), pp.1-5, 1988.

[18] S. Beji and A. B. Battjes, Experimental investigation of wave propagation over a bar, Costal Engineering, vol 19, pp.151-162, 1993.

[19] D. G. Aggelis and T. Shiotani, Experimental study of wave propagation through gouted concrete, Aci Materials Journal, vol 106(1), 2009.

[20] W. A. Thanoon, M. S. Jaafar, M. Razali, A. Kadir and J. Noorzaei, Repair and Structural Performance of Iniyially Cracked Reinforced Concrete Slabs, Construction and Building Materials, vol 19(8), pp. 595-603, 2005.

[21] V. Malenga, D. H. Zou and C. Zhang, Effects of Curing Time and Frequency on Ultrasonic Wave Velocity in Grouted Rock Bolts, Journal of Applied Geophysics, vol 59(1), pp. 79-87, 2006.

[22] L. Binda, C. Modena, G. Baronio and S. Abbaneo, Repair and Investigation Techniques for Stone Masonery Walls, Construction and Building Materials, vol 11(3), pp. 133-142, 1997.

[23] C. A. Anagnostopoulos, Laboratory Study of an Injected Granular Soil with Polymere Grouts, Tunneling and Underground Space Technology, vol 20(6), pp. 525-533, 2005.

[24] S. F. Selleck, E. N. Landis, M. L. Peterson, S. P. Shah and J. D. Achenbach, Ultrasonic Investigation of Concrete with Distributed Damage, ACI Materials Journal, vol 95(1), pp. 27-36, 1998.

[25] J. R. Rapoport, J. S. Popovics, S. V. Kolluru and S. P. Shah, Using Ultrasound to Monitor Stiffening Process of Concrete with Admixtures, ACI Materials Journal, vol 97(6), pp. 675-683, 2000.

[26] S. Rupprecht, L. G. Bennetts and M. A. Peter, Effective wave propagation along a rough thin-elastic beam, Wave Motion, vol 70, pp. 3-14, 2017.

[27] W. Flügge, Die Ausbreitung von Biegungswellen in Stäben, Z.Ang. Mathem. U. Mech., vol 22, pp. 312-318, 1942.

[28] C. Brewer, S. C. Creagh and G. Tanner, Elastodynamics on graphs-Wave propagation on networks of plates, J. of Physics A: Mathematical and Theoretical, vol 51(44), pp. 445-101, 2018.

[29] X. Li, J. Lv, Y. Luo and T. Liu, Mechanism Study on Elevation Effect of Blast Wave propagation in Hide Side Wall of Deep Underground Powerhouse, Sock and Vibration, vol 4, pp. 951-948, 2018.

[30] M. Andreou, A. Kotsoglou and S. Pantazopoulou, Moddeling Blast Effects on a Reinforced Concrete Bridge, Advances in Civil Engineering, vol 4, pp. 167-329, 2016.

[31] Y. Q. Wang, C. Liang and J. W. Zu, Examining wave propagation characteristics in metal foam beams: Euler-Bernoulli and Timoshenko models, Journal of the Brazilian Society of Mechanical Sciences and Egineering, vol 40(12), pp. 565, 2018.

[32] Z. -H. Zong, R. Zhou, X. -Y. Huang and Z.-H. Xia, Seismic response study on a multi-span

cable-stayed bridge scale model under multi-support excitations, part i: Shaking table tests, J. of Zhejiang University: Science A, vol 15(5), pp. 351-363, 2014.

[33] W. Flügge, Viscoelasticity, 2nd Edition, Springer Verlag, Berlin, 1975

[34] H. Schirmer, Über Biegewellen in Stäben, Ing. Archiv, vol 20, pp. 247-257, 1952.

[35] C. Mei, B. R. Mace, Wave Reflection and Transmission in Timoshenko Beams and Wave Analysis of Timishenko Beam Structures, Journal of Vibration and Acoustics, vol 127, pp. 382-394, 2005.

[36] G. R. Cowper, The Shear Coefficient in Timoshenko's Beam Theory, ASME J. Of Applied Mechanic, vol 33, pp. 335-340, 1966.

[37] F. Gruttmann and W. Wagner, Shear correction factors in Timoshenko's beam theory for arbitrary shaped cross-sections, Computational Mechanics, vol 27, pp.199-207, 2001.

[38] K. Terzaghi, R. B. Peck and G. Mesri, Soil mechanics in Engineering practice, 3rd ed. John Wiley & Sons, N. York, 1996.

[39] A. T. Daloglou and C. V. Vallabhan, Values of k for slab on Winkler foundation, J. of Geotechnical and Geoenvironmental Engineering, pp. 463-471, 2000.

[40] A. B. Vesic, Bending of beams resting on isotropic elastic solid, J. of Engineering Mechanics (ASCE), vol 87, pp. 35-53, 1961.